IR seeker simulator and IR scene generation to evaluate IR decoy effectiveness

Wim de Jong*, Frans A.M. Dam, Gerard J. Kunz, Ric. M.A. Schleijpen
TNO Physics and Electronics Laboratory, P.O. Box 96864, 2509 JG, The Hague, The Netherlands

ABSTRACT

IR decoys can be an effective countermeasure against IR guided anti ship missiles. However, it's not so easy to determine how the decoys should be deployed to get maximum effectiveness. A limitation of trials is that results are obtained for the specific trial condition only. Software tools have been developed to solve these problems. One solution uses recorded IR imagery from a decoy deployment trial, while the other solution generates IR imagery and is thus independent of trials. In the first solution, a combination of hardware and software is used that allows recording of a scene with an infrared camera, and simulating a missile seeker. A pre-processing algorithm corrects the recorded images before they are fed into the seeker algorithm of the simulated missile. To perform this correction the pre-processing uses the speed, distance to the target and field of view of the IR camera as fixed parameters and the speed and starting distance of the simulated missile as variable parameters. Modtran and the Navy Aerosol Model are used to calculate the atmospheric transmission effects in the pre-processing. The second solution generates artificial IR images that are subsequently fed into the seeker algorithm. This solution also allows variation of those parameters that are fixed when recorded IR imagery is used. Examples are among others: the signature of the target ship, the orientation, size and speed of the target ship, the type of decoy, the timing of the decoy sequence, atmospheric conditions etc. With these tools the effectiveness of decoy deployment in various scenarios can be evaluated.

Keywords: Scene generation, Seeker Algorithms, Infrared decoys, Atmospheric effects, Decoy effectiveness

1. INTRODUCTION

Infrared (IR) signatures of warships have been of interest for several decades. However, rather than the reduction of the signature itself, the final goal is an increase in ship survivability[1,2]. The interest in IR signature reduction must be related to the defence of ships against IR threats. Apart from signature reduction also other countermeasures (CM) as IR decoys and jammers, are essential to give protection against IR threats. In some cases a combination of signature reduction and other CM is required to counter a threat successfully.

Several factors are very important while deploying IR decoys. In case of the common used 'Walk off' technique of deploying submunitions of IR decoys not only the moment when the first submunition is deployed but also the interval between subsequent submunitions is important. For two reasons the decoys should not be fired too early. The first reason is that the decoy should burn sufficiently long to avoid re-acquisition of the ship when the decoy burns out. The safest option is to have the decoy still burning when the missile passes the ship. The second reason is that when the decoy is fired too early (when the missile is still very far away) the radiance of the decoy will stay below the threshold of the seeker due to atmospheric attenuation. The first point depends only on the remaining flight time of the missile towards the target. The second depends also on the IR visibility.
Another important point is the launch direction. Most navy ships are equipped with decoy launchers in a fixed bearing and elevation angle and a decision has to be taken which launcher is to be used to get a maximum miss distance between the missile and the ship. The ship course and speed and the wind course and speed are important factors to choose the optimum launcher. To automate the process of choosing the right launcher, course and speed, TNO-FEL has developed the EWTDA: the Electronic Warfare Tactical Decision Aid[3]. Apart from giving advice about the optimal deployment of softkill assets against radar and IR guided threats, the EWTDA also advises on course and speed, taking into account the

* Wim.deJong@tno.nl; phone +31 70 374 0438; fax +31 70 374 0654;

Technologies for Optical Countermeasures, edited by David H. Titterton,
Proceedings of SPIE Vol. 5615 (SPIE, Bellingham, WA, 2004)
0277-786X/04/$15 · doi: 10.1117/12.579500

radar cross-section of the ship, wind speed and the blind sectors of close-in weapon systems. This system is in service on the Dutch tankers and is foreseen for the Dutch frigates and LPDs.

The effectiveness of countermeasures also depends on several factors that are not under control of the target. Against an imaging seeker the decoy deployment is more critical than against a hot spot seeker. When the missile is also equipped with an RF seeker also chaff should be launched and co-located with the IR decoy.
Atmospheric conditions influence the effectiveness in different ways. The wind influences the separation between ship and decoy, while the lock-on distance, both on the target and on the decoy depends on the IR transmission through the atmosphere. The lock-on distance on the ship also depends on the ship conditions like ship signature. Decoy parameters like projected area, intensity and distance to the ship also influence the effectiveness.

Several strategies exist to determine this decoy effectiveness.
Testing the effectiveness of IR decoys against real threats, flying at a realistic missile speed and altitude is not an easy task. These threats are not available, or the risk of destroying the target is too high. Even when a harmless real threat is available only one scenario can be tested in each run with such a 'dummy' missile.
Alternatively a seeker head could be mounted to an airplane. However such an airplane, even when it is a fighter, will most probably not fly at the right altitude or with the right speed and the steering of the airplane will be very different from the steering of a real missile. With this option also only one scenario can be tested in each run.
With simulators much more scenarios can be tested. Several simulation options exist:

1. Recorded imagery versus a simulated seeker head.
2. Synthetic imagery versus a real seeker head.
3. Synthetic imagery versus a simulated seeker head.

The last option gives most freedom to change the different parameters as mentioned above and to study the effect of the different factors. At TNO-FEL work is performed at the above mentioned options 1 and 3 and both options will be discussed in this paper. In general ideal seeker conditions are used to test countermeasure effectiveness, since those conditions are most stressing for the decoys. Low clutter and good transmission are assumed to be good conditions for an IR seeker. In this paper the influence of less ideal transmission conditions will be shown and the consequences for the timing of the IR decoy submunitions.

The paper is organized as follows: Section 2 describes the different sources of IR imagery, namely recorded IR imagery, basic artificial imagery and more advanced artificial imagery. Section 3 describes the hot spot and imaging seeker algorithms. In principle both seekers can be used with the three mentioned sources of IR imagery. However not all combinations will be shown in this paper. Section 4 shows examples of simulations results that have been obtained with the combination recorded imagery / hot spot seeker, and the combination basic artificial imagery / imaging seeker. The recorded imagery originated from a static camera ashore. The advantage of the static camera is that it was at the same altitude above sea level as a sea skimming missile would fly. In a previous publication results from imagery recorded with an airplane have been reported[4]. In this paper no seeker results with the advanced artificial imagery will be reported. The final section gives conclusions and future work.

2. SOURCES OF IR IMAGERY

2.1. Recorded IR imagery

Input for the seeker simulator is a sequence of IR images of a target ship that deploys IR decoys. The ideal input for the simulator would be a sequence of images that has been recorded with a camera, sensitive in the same wavelength band as the simulated seeker that flew at the same altitude and with the same speed as the simulated threat and at the same distance from the target when the decoys are deployed. In reality IR image sequences are recorded with a camera that is mounted under an airplane that is flying with a lower speed, and usually at a higher altitude than a missile. Recordings can also be made with a camera that is not moving at all for example when it is shore based.

In the so-called pre-processing, the recorded raw image sequences are converted to images that resemble what the seeker would have seen during the fly-in. This pre-processing is necessary for several reasons, as will be described in the following paragraphs.

The speed of the airplane carrying the camera normally differs from the speed of the simulated missiles. Due to this lower speed (or zero speed for a shore based camera) the travelled distance of the camera in the direction of the target between two consecutive frames is smaller than the distance that the real missile would have travelled in the same amount of time. To clarify this effect, Figure 1 shows schematically two different situations during a simulation run. At t=0, the airplane has a certain distance to the target and the simulated missile has roughly the double distance to the target. The figures 2a and 2b show schematically what is in the FOV of the camera and the missile, assuming that the missile FOV is smaller than the camera FOV. Twenty seconds later, the airplane is closer to the target but the missile is now much closer to the target since the missile speed is much higher. This effect is even stronger for a static camera. The figures 2c and 2d show, again schematically, what is in the FOV of the camera and the missile.

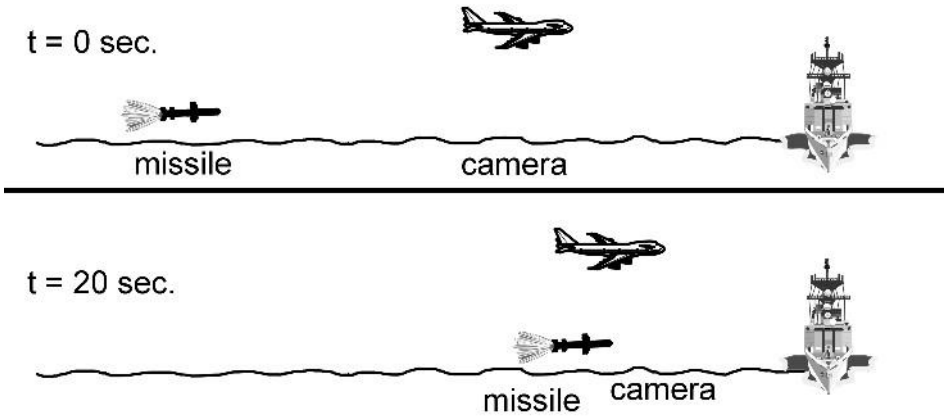

Figure 1: Schematic situation during two different phases of the simulation, showing the effect of the speed difference between the simulated missile and the airplane that carries the IR camera.

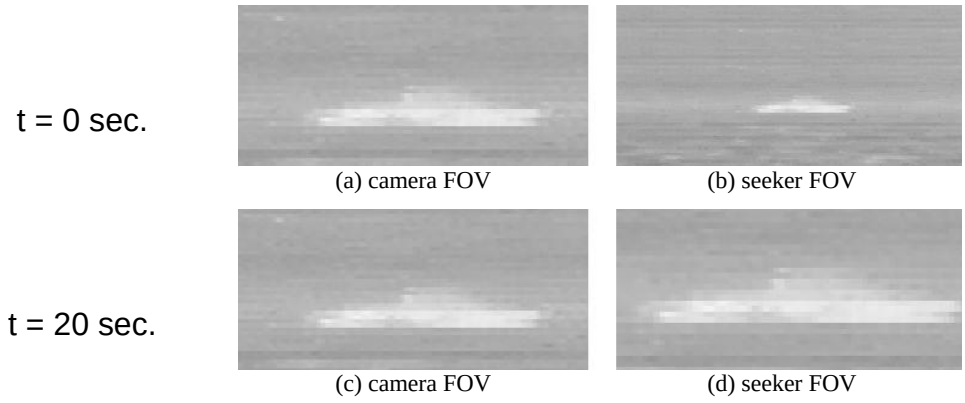

(a) camera FOV (b) seeker FOV

(c) camera FOV (d) seeker FOV

Figure 2: Indication of the IR images as seen by the camera (figure (a) and figure (c)) and the missile seeker (figure (b) and figure (d)) at the two different phases of the simulation that are schematically shown in figure 1. It is assumed that the missile FOV is smaller than the camera FOV.

To convert the recorded images, the pixels of each frame have to be remapped, taking into account the differences between the field of view (FOV) and instantaneous field of view (IFOV) of the camera and the missile, the distance difference as described above and the altitude difference. Several steps are needed in this conversion. The first step is a separation of each frame in a background (sea and sky) part and a target (ship and decoy) part. The background part and

the target part are each processed separately and combined again afterwards. The second step in the background processing is the detection of the horizon in the background images. Knowledge about the position of the horizon is necessary to be able to calculate the distance between the camera and the different parts of the sea surface that are visible in the image. This distance is used for the re-mapping of the pixels, the atmospheric correction and the determination of the position of the processed target. For these calculations the altitude of the camera is a necessary input parameter. The third step is re-mapping of the 'background' pixels in the recorded image to resemble the differences in FOV, IFOV, altitude and distance between the camera and missile. The necessity of re-mapping is already shown in Figure 2 for the target part of the images, but it also holds for the background part. The re-mapping for the sea surface and the sky background is done in different ways, since the sea surface has the curvature of the earth around the centre of the earth, while the sky background is curved around the camera.

2.1.1. Target processing steps

Target pixel re-mapping

The first step in the target processing is re-mapping of the target pixels, using the FOV, IFOV, altitude, and distance values of both the camera and the simulated missile seeker.

Depending on the difference between the camera and missile IFOV and the distance to the target of the camera and the missile this step needs a resolution modification of the original image. Figure 3 shows three different camera images during a run. The decreasing size of the squares visualizes the FOV of a simulated missile seeker for the three different distances. The camera pixels within these squares are re-mapped to the number of seeker pixels each resembling the seeker IFOV.

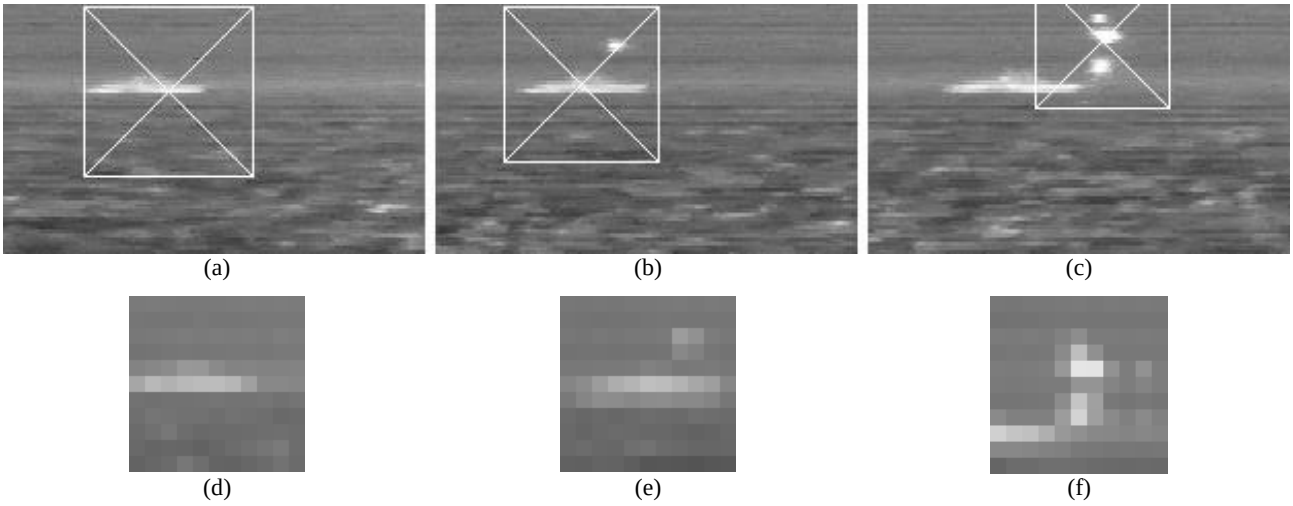

Figure 3: The first row shows camera images for three different frames (with about several seconds interval) during a specific run. The squares in these camera images indicate the size of the FOV of the missile seeker for the three simulated distances. The second row shows what is in the FOV of the missile after pixel re-mapping of the part inside the squares in the camera images that are shown in the top row.

Atmospheric correction

The second step in target processing is applying atmospheric effects to the target (ship and decoy) part. The distance between the missile and the target can be much larger than the distance between the camera and the target. (See Figure 1) The incoming IR radiation as recorded by the camera consists of radiation emitted and reflected by the target, minus part of this radiation absorbed or scattered in the path between the target and the ship, plus the radiation from the air in this path. For the extra path length, when the missile is further away than the camera, extra absorption of target radiation and extra path radiance have to be taken into account.

When this correction is not carried out, the missile detects too much contrast between the target and the background, at a distance where in reality the contrast would be very low. As a consequence, the missile would lock at the target at a

distance where lock-on is not yet possible in reality. When the missile is closer to the ship than the camera, the recorded intensity of the target is too low and has to be increased.
The transmission losses due to molecular constituents of the atmosphere are calculated using the well-known MODTRAN code (version 3.7)[5]. Transmission losses due to aerosols are calculated using the well-known Navy Aerosol Model (NAM)[6]. For these MODTRAN and NAM calculations, the atmospheric conditions, such as humidity, visibility and air temperature have to be known or otherwise estimated.
Figure 4 shows the effect of atmospheric correction in an image that was recorded from a distance of several km. The correction has only been applied to the ship, not to the sea and sky background as can be seen in the figure. Correction of the sea and sky surface is not necessary since the distance to these parts of the image is constant during the whole simulation.

(a) (b) (c)

Figure 4: Example of the effect of atmospheric correction on the image as 'seen' by the missile seeker, (before pixel re-mapping). In these images the distance from camera to ship was several km, and the distance from missile to ship was approximately twice that distance. In figure (a) no atmospheric correction has been applied. In figure (b) the correct atmospheric correction has been applied as calculated with Modtran and NAM. In figure (c) a correction has been applied based on a much lower transmission through the atmosphere.

Target position
The third step in target processing is a calculation where the ship should be placed back in the processed background, relative to the horizon. If the missile is flying very low and the distance to the ship is larger than the distance to the horizon the ship should be placed behind the horizon. This means that the lower part of the ship is not visible for the missile.
If on the opposite the missile is flying relatively high and has come close to the ship, the missile sees the ship before the horizon, with a sea background. Somewhere in between the ship should be placed exactly at the horizon. The position of the horizon has been calculated in the background processing.

The final pre-processing step is combining the processed target and processed background part for each frame in the sequence. At this point sharp edges between the target and the background should be avoided. This step has already been performed in the images that are shown in Figure 3 and Figure 4.

2.2. Basic synthetic imagery

In the basic synthetic imagery the ship consists of four stacked 'shoe boxes'; the hull, the super structure, the funnel and the plume. Each box has its own dimensions and can be placed relative to the ship position. The port and starboard side of the ship can have different fixed temperatures. The temperature of bow and stern sides are the average of these two. The boxes are designed to be put on top of each other and be viewed from low elevations. A simple plume alignment with the ship length-axis is assumed, ignoring effects of cross winds.
The sky background has a uniform temperature T_{air}. The sea surface has a temperature T_{sea} and a clutter temperature ΔT_{sea}. This clutter in the sea background is random and has no correlation in time and space. The propagation through the atmosphere is defined by the extinction coefficient σ. It is possible to define three different values of σ, one used for the ship and the background radiation, the other two are for the plume and flares respectively. This definition is far less detailed than the procedure for the recorded imagery that is described above and the high quality synthetic imagery that is described below.
The IR-decoy submunitions are defined by cubes with a dimension that is time dependent. The radiance of each submunition is also time dependent. The number of submunitions is not limited and each submunition can independently be placed and has its own fall speed.

2.3. High quality synthetic imagery

To improve the quality of the synthetic imagery the EOSTAR / ARTEAM model suite[7-9] will be used. The core capability of the EOSTAR application is to provide accurate visualization of image distortion due to refraction effects in the atmosphere. This model suite incorporates the Electro-Optical Signature Model (EOSM) of the TNO Physics and Electronics Laboratory for signature calculations of the target[2]. Infrared signature prediction is performed with a first principles code, which solves the heat balance equation for an object on the sea surface. All relevant heat fluxes, such as convective heat exchange with the ambient air, irradiation from the sun, sea and sky in both shortwave and longwave bands, are included, as well as the physical properties of the target construction. The code relies on MODTRAN for the computation of atmospheric (sky) radiance and solar irradiance.

To create a more realistic background than is used in the basic synthetic imagery EOSTAR / ARTEAM will be updated with the Marine Infrared Background Simulator (MIBS) of the TNO Physics and Electronics Laboratory[10]. MIBS creates realistic 3-5 and 8-10 micron broadband calibrated infrared simultaneous clutter backgrounds of a maritime scene. The scene contains sea, horizon and sky. It may also contain clouds. Image sequences of any length can be simulated with clutter behaviour adjusted for the selected frame rate.

For the purpose of decoy effectiveness studies, EOSTAR generates the image as seen by the missile seeker under the prevailing environmental conditions (transmission, refraction, turbulence, etc), taking into account the actual viewing direction and resolution of the seeker head. If a target is present in the scene, the target signature is also evaluated and taken into account. The image as seen by the seeker can be displayed on the screen.

In addition, a special EOSTAR version has been extended with a module that allows ships to fire decoys in various sequences and for various scenarios (see Figure 5). This module has been customized for the Dutch frigates, but can be tailored to accommodate other platforms. The platform under attack and the effects of firing decoys can be visualized (see Figure 6). The actual position of the decoys is evaluated incorporating the ship's motion (course, speed, pitch and roll), and the prevailing wind speed and direction. The figure shows a snapshot of the deployment of decoys from an arbitrary viewing angle in missile seeker resolution. Figure 7 shows refraction effects on images of a target deploying decoys. The figure shows snapshots of the deployment of decoys from an arbitrary viewing angle for different atmospheric conditions. For the purpose of illustrating the refraction effects, the resolution in these images might not be the same as can be expected for an imaging missile.

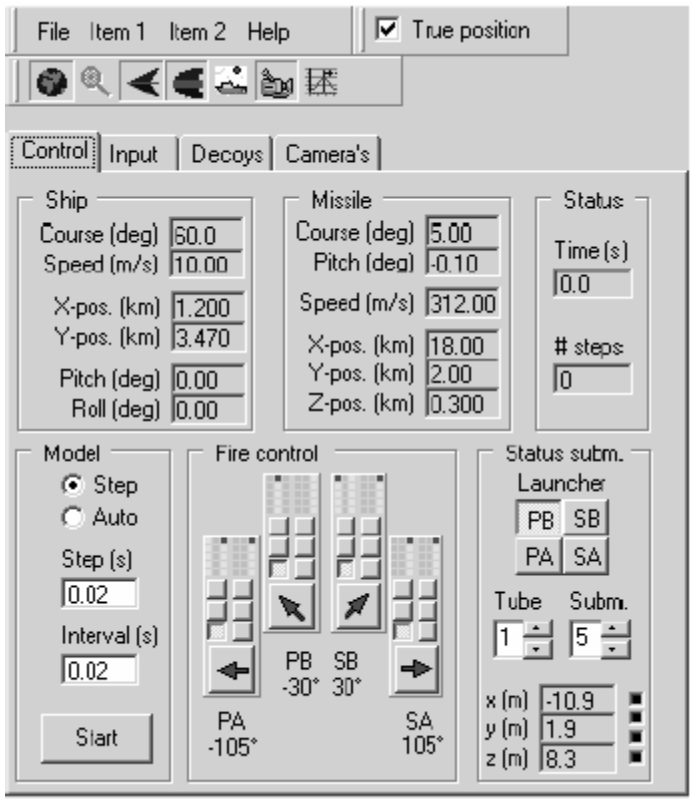

Figure 5: Example of the EOSTAR module that allows ships to fire decoys for various fire control and ship/missile altitude scenarios. This module has been customized for Dutch naval units, but can be tailored to accommodate other platforms.

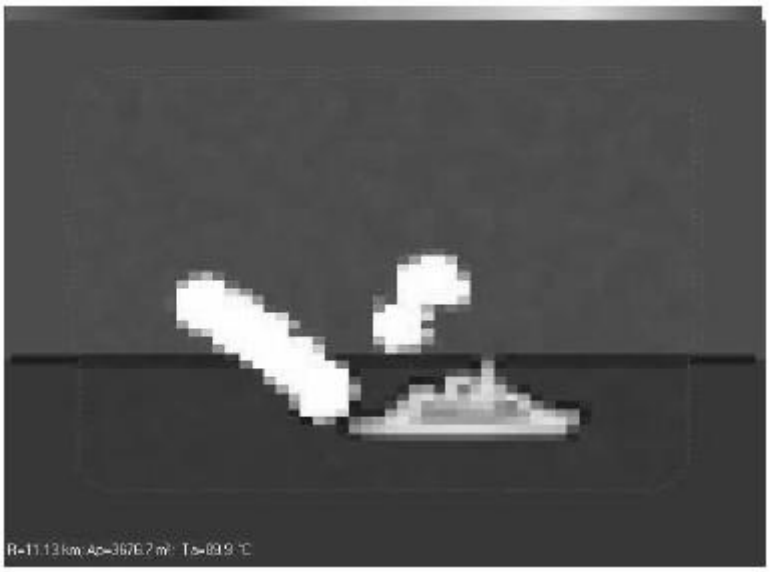

Figure 6: Visualisation of the platform under attack and the effects of firing decoys. The figure shows a snapshot of the deployment of decoys from an arbitrary viewing angle in missile seeker resolution.

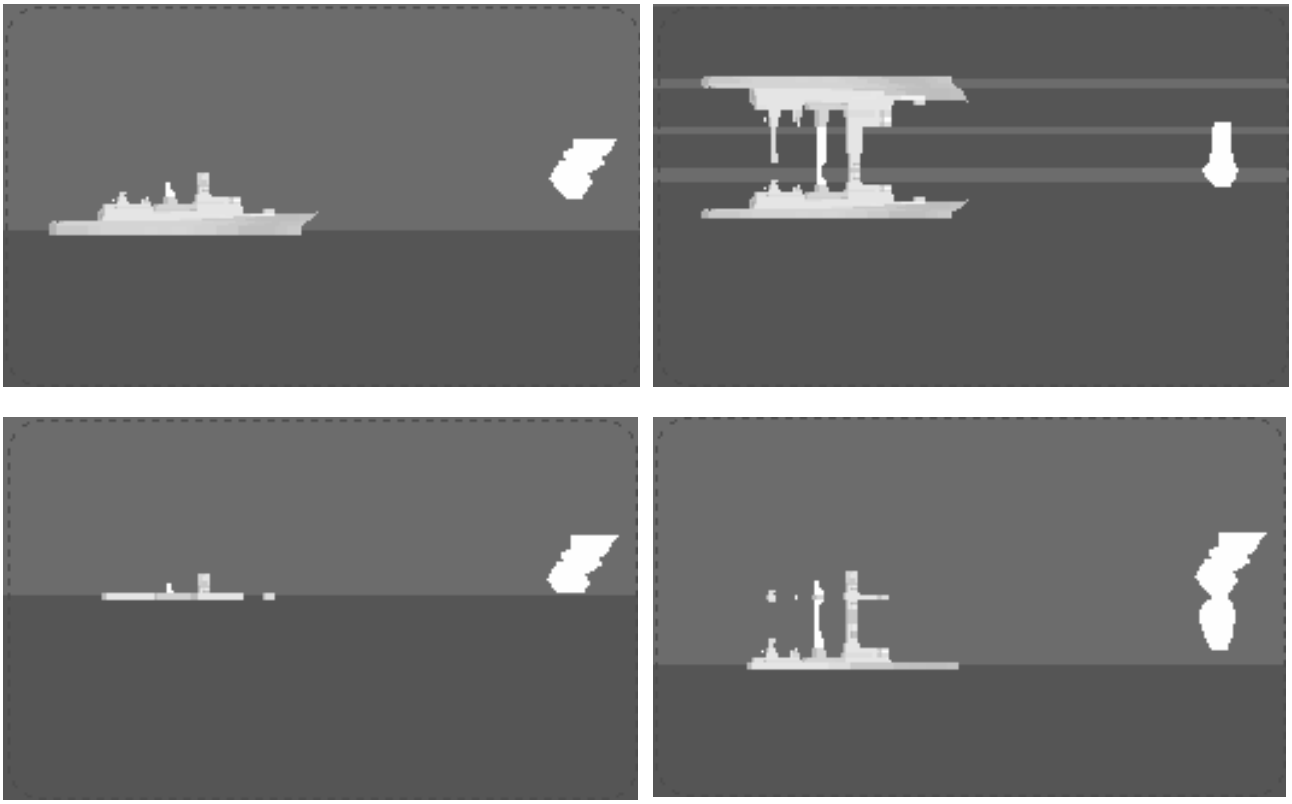

Figure 7: Visualisation (with possibly a higher resolution than is expected for an imaging missile) of atmospheric refraction effects. The figure shows snapshots of the deployment of decoys from an arbitrary viewing angle for different atmospheric conditions.

3. SEEKER ALGORITHMS

3.1. Hot Spot seeker

A software model has been developed that simulates a hot spot missile seeker. The variable parameters that can be fed into the simulation are the speed, altitude, and starting distance of the missile.

This seeker has a search and a track mode. The scanning detector element is simulated by an 11 x 11 pixel array to determine the location of the hottest part of the target within the missile's field of view. The values for the variable simulation parameters flying speed, flight altitude and starting distance are already used in the pre-processing for the pixel re-mapping and atmospheric correction.

Once the missile has been launched the simulated seeker starts the search mode. Within the field of regard of the missile a scan pattern is followed. The scan pattern is positioned around the horizon in the images. Within each exposure the seeker determines the centre of gravity of the intensity within the field of view. If the contrast radiance within the field of view exceeds a pre-defined detection threshold, the seeker goes into track mode. In the track mode the field of view is smaller than that for the search mode. For each exposure the hottest spot is determined within its field of view and the missile is directed towards that point. The field of view of the next exposure is centred on that position. Note that mechanical inertia in the seeker gimbal is ignored. This is a reasonable approach for this seeker and creates the worst case situation from the decoy point of view. If the track is lost, the missile returns to the search mode after a pre-defined dead-reckon time has expired.

The output of the simulation consists of several parts. The first output is an image sequence with the image as seen by the missile seeker after atmospheric correction and pixel re-mapping. In this sequence the FOV and aim point of the seeker is indicated by a square with a reticule. The second output is a log file with the distance between the aim point of the seeker and the centre of the ship during the whole simulation. The behaviour of the simulated hot spot seeker has been compared with the behaviour of an existing hot spot seeker. The results of this comparison show that both seekers lock at the same target almost at the same time and for the same period.

3.2. Basic Imaging seeker

The currently implemented imaging seeker is relatively simple and is characterized by the horizontal and vertical instantaneous FOV (IFOV), the number of pixels in horizontal and vertical direction, the wavelength range, sensitivity in the form of *NETD*, and the frame rate, with which the seeker processes are performed.
The first step is digitising the image with a given number of bits, where part of the range between the smallest and the largest intensity is linearly mapped on 2^{nbits} grey levels. From this a second, thresholded binary image is produced. The threshold level is determined for each horizontal line in the image separately to be able to use different thresholds against a sky or a sea background. After thresholding a binary image is produced in which the pixels above the threshold have the value 0 and all others the value –1.
In the next step all pixels that are above the threshold and also connected to neighbouring above threshold pixels (horizontally, vertically or diagonally) will be given the same index number. The output is a bitmap where each pixel has either the value –1 or a value from 1 to n where n is the total number of blobs in the image. The blob finding can be limited to a given window.
In the third step for all blobs with more than a certain minimum number of pixels, a number of parameters will be determined. Currently only the number of pixels in the blob and the size of a rectangular window that fits around the blob are used for finding the largest blob and setting the track window respectively. Other blob parameters like width/height ratio or average intensity can be used in the future for improving the counter-counter measure capabilities of the tracker.
During acquisition an azimuth scan is made and the angular position of the largest (in number of pixels) target is marked. At the end of the scan the seeker slews to this position and starts tracking. The track window is a rectangular box, fitting around the largest blob with a preset margin on all four sides. This window is used in the next frame for finding blobs. Blobs, e.g. from decoys, outside the track window are ignored in the tracking. Blobs that enter the track window are ignored unless they are connected with the blob inside that track window that is currently tracked. At that instant the track window is enlarged to fit the new larger blob. The tracking errors in elevation and azimuth are determined by the distance between the centre of the focal plane array and the centre of the tracking window defined above.

4. SIMULATION RESULTS

4.1. Hot spot seeker with recorded IR imagery

From a static platform several decoy runs of a ship that was using submunitions to create a walk-off pattern were recorded.
In the simulations two parameters have been varied.

1. The distance between the missile and the ship at time t = 0, which is the time when the first submunition is deployed. This distance varies over a range of more than 10 km.
2. The atmospheric transmission, which was chosen to be a normal atmosphere or an atmosphere with a low visibility.

Figure 8 shows two screenshots during a simulation several seconds after firing the last submunition. Some earlier deployed submunitions are still visible. The left hand side shows the situation with normal visibility and the right hand side shows the low visibility condition. In the far left of both images the plume of the target ship is visible. In the situation with normal visibility the seeker is locked on the decoys. In the situation with low visibility the seeker is still searching, since the intensity of the decoy does not exceed the seeker threshold in this situation with high atmospheric attenuation. It can be concluded that in this situation the decoy was fired much too early and valuable burning time of the decoy is lost.

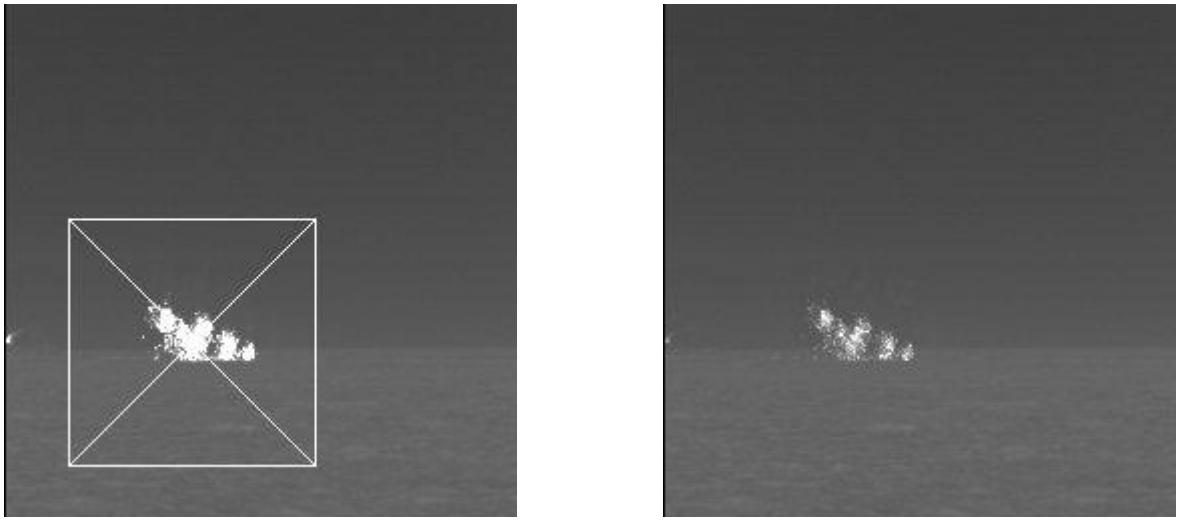

(a) (b)

Figure 8: Screenshots from a simulation with a hot spot seeker and recorded IR imagery. Figure (a) shows results with normal visibility, figure (b) shows the result at the same time during the simulation with low visibility. In both cases the decoys were fired at the same time. In the situation with good visibility the seeker immediately locked on the decoys. However in the case with poor visibility the decoy was fired too early, when the missile is still too far away. The intensity doesn't reach the seeker threshold and the seeker is still searching while valuable burning time of the decoy is lost.

Figure 9 shows two screenshots during a simulation at the end of the expected burning time of the last fired submunition. The left hand side shows the situation with normal visibility and the right hand side shows the low visibility condition. In the left side of both images the plume of the target ship is visible. In the situation with normal visibility the seeker is still locked on the decoys. However in the situation with low visibility the lock was broken and the seeker started searching again. Since the target ship is still in the vicinity of the decoys the seeker will most probably find the ship and will lock on it. It can be concluded that also in this situation the decoy was fired too early since the effective burn time is lower in situations with poor visibility.

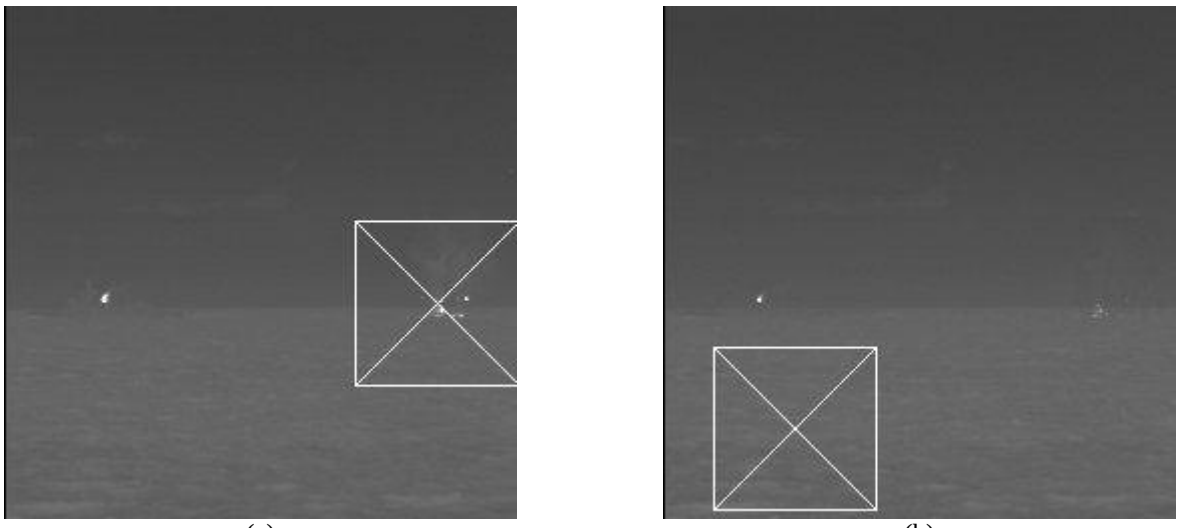

(a) (b)

Figure 9: Screenshots from a simulation with a hot spot seeker and recorded IR imagery. Figure (a) shows results with normal visibility, figure (b) shows the result at the same time during the simulation with low visibility. In both cases the decoys were fired at the same time. The images are taken at the end of the burning time of the decoys.

It can be concluded from these simulations that in the case of low visibility the decoys should be fired later than in the case with good visibility for two reasons. The first reason is that the detection distance is shorter in low visibility conditions, not only for the target ship, but also for the decoys. The second reason is that in low visibility conditions the time during which the decoy radiance is above threshold is (much) lower.

4.2. Hot Spot versus Imaging

Two results from the imaging seeker with artificial imagery will be shown. In the first example the decoys were deployed in a common used walk-off pattern that is primarily designed for the seduction of a hot spot seeker. In the second example a more advanced decoy deployment is used.
In the first example the decoys are placed in the field of view of the imaging seeker. However the missile disregards the decoy submunitions since they do not form a connected blob that is larger than the ship and this imaging seeker does not look for the brightest spot, but for the largest blob. In figure (b) the submunitions become connected, but since this happens outside the track window this large blob is ignored by the seeker. As a consequence this decoy deployment is not effective against this imaging seeker.

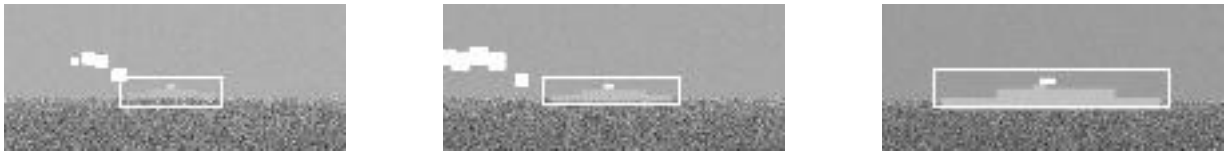

(a) (b) (c)

Figure 10: This figure shows screenshots at three different times during an engagement. The ship has fired 'conventional' decoys with a so-called walk-off pattern to break the lock-on. Figure (a) already shows that the track window of the imaging seeker doesn't include the decoys since they are not a valid target for this imaging seeker. The reason is that the submunitions are not connected and this imaging seeker uses the size of the target as a criterion. In figure (b) the submunitions become connected, but since this happens outside the track window this large blob is ignored by the seeker.

In the second example the decoys are also placed in the field of view of the seeker, but now the submunitions are placed closer to the ship. Now the decoy cloud forms one blob with the target itself. When the decoy cloud and the ship become separated, the seeker will choose that largest blob and will follow the decoy cloud.

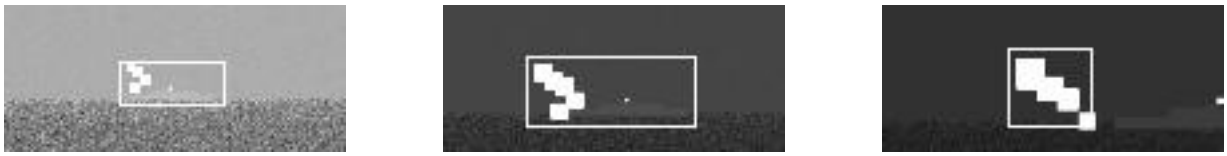

(a) (b) (c)

Figure 11: This figure shows screenshots of an engagement that are taken at the same three different times as the screenshots that are shown in Figure 10. In this situation the ship has fired the decoys closer to the ship, which gives a connected decoy cloud. Figure (a) shows that the track window of the imaging seeker includes the ship and the decoys since they are connected. The same holds for the track window in figure (b). In figure (c) the seeker follows the decoy cloud since the projected size is larger than that of the ship.

5. CONCLUSIONS

To study decoy effectiveness several simulation strategies exist. This paper discussed two of them, the first using recorded IR imagery and the second using artificial imagery. Both strategies use simulated seekers, of which a hot spot and an imaging seeker are available. Since a flying missile seeker with a variable speed and variable starting distance is simulated, the recorded images, from a static camera or a camera moving at relatively low speed, are corrected before they are fed into the seeker algorithm of the simulated missile. To perform this correction the pre-processing uses the speed, distance to the target and field of view of the IR camera as fixed parameters and the speed and starting distance of the simulated missile as variable parameters. MODTRAN and the Navy Aerosol Model are used to calculate the atmospheric transmission effects in the pre-processing.

Examples show how recorded data is used to simulate a missile with a hot spot seeker approaching a ship deploying decoys. In these examples the effects of different atmospheric conditions on the seeker behaviour is shown.
It can be concluded that the correct timing of the submunitions depends on the atmospheric conditions. Firing intervals that are effective for a situation with good visibility appear to be ineffective in a scenario with low visibility.
To demonstrate the second solution an imaging seeker model with relatively simple algorithms was implemented and very basic images were generated. The effectiveness of traditional walk-off decoys was compared with more advanced decoy systems. The results show that against this imaging seeker model a common used walk-off pattern is not effective to break the lock-on. It can be concluded that against this imaging seeker the geometry of the decoy deployment is much more important than against a hot spot seeker.
Medium term plans are the implementation and validation of a more advanced imaging seeker model and implementation of more advanced atmospheric effects such as refraction, turbulence and blur in the high quality synthetic imagery. On a longer term the implementation of dual band (Long Wave IR and Mid Wave IR) and/or dual mode seekers (IR and Radar) are foreseen.

ACKNOWLEDGMENTS

The development of the missile simulator is sponsored by the Royal Netherlands Navy through assignment A99KM615. The authors acknowledge the support of A.M.J. van Eijk in MODTRAN and NAM calculations.

REFERENCES

1. H.M.A. Schleijpen, “Evaluation of infrared signature suppression of ships”, in *Targets and Backgrounds: Characterization and Representation II*, W.R. Watkins, and D. Clement, Editors, Proceedings of SPIE Vol. 2742, p. 245-254 (1996).
2. F.P. Neele, and W. de Jong, “Prewetting systems as an IR signature control tool”, in *Targets and Backgrounds VIII: Characterization and Representation*, W.R. Watkins, D. Clement, and W.R. Reynolds, Editors, Proceedings of SPIE Vol. 4718, p. 156-163 (2002).
3. http://www.tno.nl/instit/fel/div2/prod/ewtda.html
4. W. de Jong, S.P. van den Broek, R. van der Nol, “IR seeker simulator to evaluate IR decoy effectiveness", in *Targets and Backgrounds VIII: Characterization and Representation*, W.R. Watkins, D. Clement, and W.R. Reynolds, Editors, Proceedings of SPIE Vol. 4718, p. 164-172 (2002).
5. F.X. Kneizys, L.W. Abreu, G.P. Anderson, J.H. Chetwynd, E.P. Shettle, A. Berk, L.S. Bernstein, D.C. Robertson, P. Acharya, L.S. Rothman, J.E.A. Selby, W.O. Gallery and S.A. Clough, *The Modtran 2/3 report and Lowtran 7 model*, Philips Laboratory PL/GPOS, Hanscom AFB, MA, 1996.
6. S.G. Gathman, “Optical properties of the marine aerosol as predicted by the Navy Aerosol Model”, *Opt. Eng*. **22**, pages 57-63, 1983.
7. G.J. Kunz, M.M. Moerman, A.M.J. van Eijk, S.M. Doss-Hammel, D. Tsintikidis, “EOSTAR: an electro-optical sensor performance model for predicting atmospheric refraction, turbulence, and transmission in the marine surface layer”, in *Optics in Atmospheric Propagation and Adaptive Systems VI*, John D. Gonglewski, and Karin Stein, Editors, Proceedings of SPIE Vol. 5237, p. 81-92 (2003).
8. G.J. Kunz, M.A.C. Degache, M.M. Moerman, A.M.J. van Eijk, F.P. Neele, S.M. Doss-Hammel and D. Tsintikidis, “Status and developments in EOSTAR, a model to predict IR sensor performance in the maritime environment”, in *Optics in Atmospheric Propagation and Adaptive Systems VII*, John D. Gonglewski, and Karin Stein, Editors, Proceedings of SPIE Vol. 5572, p. 101-111 (2004).
9. http://www.tno.nl/eostar.html
10. P.B.W. Schwering, “Maritime infrared background clutter”, in *Targets and Backgrounds: Characterization and Representation II*, W.R. Watkins, and D. Clement, Editors, Proceedings of SPIE Vol. 2742, p. 255-266 (1996).